analytical chemistry

Subscriber access provided by UNIV OF CALIFORNIA SAN DIEGO LIBRARIES

Article

Characterization of Intact Antibody Drug Conjugate Variants using Microfluidic CE-MS

Erin A Redman, John Scott Mellors, Jason A. Starkey, and J. Michael Ramsey

Anal. Chem., **Just Accepted Manuscript** • DOI: 10.1021/acs.analchem.5b03866 • Publication Date (Web): 14 Jan 2016

Downloaded from http://pubs.acs.org on January 16, 2016

Just Accepted

"Just Accepted" manuscripts have been peer-reviewed and accepted for publication. They are posted online prior to technical editing, formatting for publication and author proofing. The American Chemical Society provides "Just Accepted" as a free service to the research community to expedite the dissemination of scientific material as soon as possible after acceptance. "Just Accepted" manuscripts appear in full in PDF format accompanied by an HTML abstract. "Just Accepted" manuscripts have been fully peer reviewed, but should not be considered the official version of record. They are accessible to all readers and citable by the Digital Object Identifier (DOI®). "Just Accepted" is an optional service offered to authors. Therefore, the "Just Accepted" Web site may not include all articles that will be published in the journal. After a manuscript is technically edited and formatted, it will be removed from the "Just Accepted" Web site and published as an ASAP article. Note that technical editing may introduce minor changes to the manuscript text and/or graphics which could affect content, and all legal disclaimers and ethical guidelines that apply to the journal pertain. ACS cannot be held responsible for errors or consequences arising from the use of information contained in these "Just Accepted" manuscripts.

ACS Publications

Analytical Chemistry is published by the American Chemical Society. 1155 Sixteenth Street N.W., Washington, DC 20036

Published by American Chemical Society. Copyright © American Chemical Society. However, no copyright claim is made to original U.S. Government works, or works produced by employees of any Commonwealth realm Crown government in the course of their duties.

Characterization of Intact Antibody Drug Conjugate Variants using Microfluidic CE-MS

Erin A. Redman[1], J. Scott Mellors[5], Jason A. Starkey[6], J. Michael Ramsey[1,2,3,4]

[1]Department of Chemistry, [2]Department of Applied Physical Sciences, [3]Department of Biomedical Engineering, [4]Carolina Center for Genome Sciences, University of North Carolina, Chapel Hill, North Carolina 27599, United States; [5]908 Devices Inc., Boston, Massachusetts, United States; [6]Pfizer Inc., Chesterfield, Missouri, United States

ABSTRACT

In this work we utilize capillary electrophoresis-mass spectrometry (CE-MS) in an integrated microfluidic platform to analyze an intact, lysine-linked antibody drug conjugate (ADC) in order to assess post translational modifications and drug load variants. The initial charge heterogeneity of the unconjugated IgG-2 monoclonal antibody (mAb) was assessed by separating intact charge variants. Three main charge variants were resolved in the CE dimension. These variants were attributed to pyroglutamic acid formation and decarboxylation on the primary structure of the mAb through characteristic mass shifts and changes in electrophoretic mobility. Additionally, glycoforms of the antibody charge variants were identified in the deconvoluted mass spectra. The observed glycoforms and their distribution compared favorably to a released N-glycan analysis performed on the mAb. After conjugation, the ADC was analyzed using the same microchip CE-MS method. The addition of a drug load resulted in a decrease in mobility and an increase in mass of 3145 Da. Five main species that differed in their respective drug-to-antibody ratios (DAR) were fully resolved in the CE separation, with each DAR displaying the same variant population observed on the unconjugated mAb. A DAR range of 0-4 was observed with an average of 1.7 drug loads. The DAR distribution generated from the microfluidic CE-MS data compared favorably to results from infusion-ESI-MS and imaging CE (iCE) analysis of the ADC, techniques commonly used for intact mAb and ADC characterization.

INTRODUCTION

Antibody drug conjugates (ADCs) are monoclonal antibodies (mAbs) decorated with highly potent small molecule drugs that generally have anti-tumor activity. This class of biotherapeutic has drawn particular interest in the biopharmaceutical industry due to their potential ability to harness the specificity of a mAb and the therapeutic value of a chemotherapeutic drug.[1–6] The importance of, and challenges associated with characterizing biotherapeutic mAbs have been thoroughly described and the difficulty and complexity of these challenges are further exacerbated in the case of ADCs due to their increased heterogeneity.[1,7–11]

Typically, ADCs are manufactured in a process that couples a smaller drug molecule to a mAb, via a linker.[1,5,6] The primary mAb by itself will exhibit heterogeneity due to post translational modifications and degradation that commonly occurs during cellular expression, processing, and in storage. The complexity of the mAb molecule increases further following conjugation to generate the ADC. Various approaches and technologies have been demonstrated to couple the mAb and drug molecule, but regardless of the conjugation chemistry used, the resulting ADC population is often a diverse mixture of species in terms of the drug-to-antibody ratio (DAR) and their isoforms. Thus, the variants in the ADC population include the initial variants of the primary mAb molecule layered with additional heterogeneity introduced as a result of the conjugation process.

The various DAR species of an ADC can potentially exhibit very different pharmacokinetic properties.[1,3,6,12,13] As such, the DAR and often the distribution are deemed as being critical quality attributes of an ADC. At the intact level, analyses of these species are often accomplished using separation techniques such as hydrophobic interaction chromatography (HIC), ion exchange chromatography (IEC), reverse phase liquid chromatography (RPLC), capillary electrophoresis (CE), or capillary isoelectric focusing.[1,2,11,14–21] These approaches are coupled to absorbance-based detection techniques and are generally incompatible with mass spectrometry due to the high salt content required for analysis. RPLC can be interfaced with a mass spectrometer as a desalting technique to generate an infusion-like spectrum of the intact ADC sample, but separation of variants does not occur.[17,22–24] Recently, several studies have been published using native spray ion mobility spectroscopy (IMS) with MS detection for characterizing ADCs.[25–27] With this approach, DAR and distribution can be determined from the mass spectrum and some resolution between DAR species is obtained during the IMS separation. However, a specialized MS instrument with IMS capabilities is necessary.

Recently we described a method for assessing the charge heterogeneity of intact mAbs using microfluidic CE-ESI with online MS analysis.[28] With very little sample preparation, charge variants of mAbs can be separated and introduced directly into the mass spectrometer via ESI. Having the CE separation prior to MS analysis generates electrophoretic mobility data that can be used in conjunction with mass data as criteria for identifying mAb charge variants. Additionally, the CE separation prior to MS analysis simplifies the resulting mass spectra. In this

work we demonstrate the use of this method for measuring both charge variant heterogeneity and DAR distribution of an ADC at the intact level. While DAR and distribution have been characterized using infusion-MS or separation techniques coupled to optical detection, this is the first example of a solution phase separation of intact ADC species with direct MS detection to characterize charge variant heterogeneity, and DAR distribution.

EXPERIMENTAL SECTION

Materials and Reagents. Deionized water was generated with a Nanopure Diamond water purifier (Barnstead International, Dubuque, IA). Optima LC/MS grade 2-propanol and acetic acid (99% purity) were obtained from Fisher Scientific (Fairlawn, NJ). The silane coating reagent 3-(aminopropyl)di-isopropyl-ethoxysilane (APDIPES) was purchased from Gelest (Morrisville, PA) and the methyl-terminated polyethylene glycol *n*-hydroxy succinimide ester (NHS-PEG_{450}) was purchased from Nanocs Inc. (Boston, MA). Trichloro-(1H,1H,2H,2H-perfluorooctyl)-silane was purchased from Sigma-Aldrich (St. Louis, MO). The monoclonal antibody mAb-A and the monoclonal antibody conjugate mAb-Ac were provided by Pfizer Inc. (St. Louis, MO).

Sample Preparation. Monoclonal antibody samples were stored in their respective formulation buffers at -20 °C until analysis. Samples were thawed at room temperature and diluted to 0.5 mg/mL for mAb-A and 1.0 mg/mL for mAb-Ac with an aqueous solution of 10% 2-propanol 0.2% acetic acid (pH 3.17). The mAb samples were then buffer exchanged to 10% 2-propanol 0.2% acetic acid using an Amicon Ultra Ultracel 50 kDa centrifugal filter (Millipore, Billerica, MA). The final sample volume was 100 µL for both mAbs.

Fabrication and Preparation of Microfluidic Devices. The design for the CE-ESI devices has been described previously[28,29] and incorporates an injection cross for sample handling, a 23-cm long separation channel with asymmetrically tapered turns[30–34], an electroosmotic pump for sustaining ESI, and an integrated ESI emitter.[35,36] Standard photolithography and wet chemical etching techniques were used to fabricate the CE-ESI devices in house from 0.55-mm thick D263 glass wafers (Telic Co., Valencia, CA). The integrated ESI emitter was formed by dicing the corner of the device to 90° using a precision dicer from Disco Technologies (Santa Clara, CA) and then polishing the edges of the emitter with 3 µm cerium oxide abrasive lapping paper and a lapping wheel (Ultra Tec, Santa Ana, CA). Buffer reservoirs with a liquid capacity of 200 µL were formed by attaching 8-mm diameter glass cylinders to the devices with epoxy (Loctite E-120HP, Henkel Corporation, Germany).

As described previously, CE-ESI devices were coated with an aminopropylsilane reagent and a polyethyleneglycol (PEG) reagent to reduce analyte adsorption and suppress EOF.[28,29] Briefly, the device was coated with APDIPES via chemical vapor deposition[29] and then the injection cross and separation channels were covalently coated with an NHS-PEG_{450} reagent.[28] After the coating procedures were completed, 5 µL of trichloro-(1H,1H,2H,2H-perfluorooctyl)-

silane was applied to the ESI emitter to increase the hydrophobicity of the external surface and facilitate ESI.

CE-ESI-MS Device Operation and Data Analysis. CE-ESI devices were operated by applying voltage to the solvent reservoirs via platinum wire electrodes. The electrodes were powered by an in-house built power supply containing five high-voltage modules (UltraVolt , Ronkonkoma, NY): Three 0 to +35 kV modules (P/N 35A24-P15) to power Sample, BGE, and Sample Waste reservoirs (Figure 1), and two 0 to +10 kV modules (P/N 10A12-P4) to power the EO pump reservoir and the ESI shield electrode. The voltage output of the power supply was controlled via a custom LabVIEW (National Instruments, Austin, TX) program. An aqueous solution of 10% 2-propanol 0.2% acetic acid (pH 3.17) was used for all analyses. As denoted by the arrows in Figure 1, devices were operated such that mobile cations migrate against the suppressed anodic EOF in the PEGylated channels. A gated injection scheme was used for sample manipulation and injection.[29,37] Typical voltages for operating the CE-ESI devices are provided in Table 1. Injection of the sample was performed by switching the voltage profile from the gated state to the injection state for 200 ms and back again. Infusion of mAb-Ac was performed by allowing the voltages to remain in the injection state.

Table 1: Representative voltage scheme for gated injections on the CE-ESI device.

	Applied Voltage (kV)	
	Gate	**Inject**
Sample	20	20
BGE	20	19
Sample waste	18	19
EO pump	1	1
Shield	0.5	0.5

Devices were positioned in front of the inlet of the mass spectrometer using a stage built in house.[28] MS analysis was performed using a Waters LCT-Premier time-of-flight mass spectrometer (Waters Corporation, Milford, MA) operated in V-mode with the source at 105 °C. Data were acquired over a mass range of 4000-6000 m/z with a 0.2 s scan time. Deconvolution of the mass spectra was performed based on maximum entropy analysis using the MaxEnt1 deconvolution algorithm in the MassLynx software as described previously.[10,28,38,39]

RESULTS AND DISCUSSION

Analysis of mAb-A Variants. The monoclonal antibody mAb-A is an IgG-2 antibody. Intact analysis of mAb-A charge variants via microfluidic CE-ESI-MS revealed three main variants of the mAb (labeled 1, 2, and 3) as seen in Figure 2a. To generate mass spectra for the charge variants, the mass scans were averaged over the width of the CE bands. The mass spectrum of the most abundant charge variant in the separation is provided in Figure 2b. Masses for the

charge variants were obtained through deconvolution of the mass spectra and are provided above their respective bands in Figure 2a.

Preliminary identification of the charge variants was accomplished by considering both the mass shift and relative change in electrophoretic mobility between variants. More detailed information about the migration times and apparent mobilities of the charge variants can be found in Table S1 of the Supporting Information. The mass difference between the two most abundant charge variants, 2 and 3, is 18 Da, which is similar to the mass shift attributed to multiple common modifications including oxidation and pyroglutamic acid formation at the N-terminus of the heavy chain.[7] While both modifications are plausible, pyroglutamic acid formation is more consistent with the observed shift in electrophoretic mobility because there is a reduction in charge associated with the cyclization reaction with the N-terminal amine. The presence of this modification was confirmed using conventional peptide mapping with MS detection by collaborators at Pfizer (data not shown). With this analysis strategy where mobile cations are sampled, the most mobile variants in the electropherogram (those with the lowest migration time) are more positively charged, or more basic, than those with longer migration times. Thus, the mAb-A charge variant 2 is more basic than the more abundant variant 3. The apparent mobility of variants 2 and 3 are 2.47×10^{-4} cm^2/Vs and 2.44×10^{-4} cm^2/Vs, respectively. This is a mobility decrease of 0.03×10^{-4} cm^2/Vs. Considered with respect to pyroglutamic acid formation the decrease in mass of 18 Da is consistent with the decrease in mobility due to the loss of +1 charge. The same mobility shift of 0.03×10^{-4} cm^2/Vs between mAb bands was previously observed for C-terminal lysine variants, which also differ by 1 charge unit.[28] Thus, this mobility shift has twice been found to be characteristic of mAb modifications that alter the net charge by 1 with relatively minor mass changes.

The most basic variant at 149135 Da (band 1 in Figure 2a) is lower in mass than both other charge variants. There is a mass shift of 44 Da between this variant and its more acidic neighbor (band 2) and the magnitude of the mobility shift suggests that the modification also induces a change in net charge of 1. These properties agree with the mass and charge modifications characteristic of a decarboxylation event; removal of a carboxylic acid group as carbon dioxide results in a mass decrease of ~44 Da and elimination of a negative charge. A mAb species with this modification would appear as more basic and 44 Da lighter in mass. As such, we have attributed the most basic variant of mAb-A to be a decarboxylated form of the molecule. While the discussion of charge variants here has been based on the addition or removal of charged residues from the mAb structure, it has been shown that other types of modifications, such as oxidation, can affect the net charge of a mAb by altering the pKa of neighboring residues.[11] Further experiments are needed to assess the impact such modifications may have on this analysis and how they manifest in the separation.

With this analysis, a sufficient level of sensitivity and resolution was obtained in the mass domain to detect several glycoforms of mAb-A. Glycosylation is an expected modification of monoclonal antibodies, but does not induce a change in net charge unless sialic acids are present.[7] Thus, the mAb-A glycoforms are expected to cause a characteristic shift in mass, but

not a mobility shift. Identified mAb-A glycoforms are labeled in the deconvoluted mass spectrum in Figure 2c. It should be noted that the glycoform masses generated during intact analysis account for the glycans on both heavy chains of the mAb. As such, it is not possible to differentiate between some glycoforms that have identical masses, such as G0F/G2F and G1F/G1F. The glycoforms identified are characteristic of Chinese hamster ovary expressed monoclonal antibodies. Based on the areas of the mass peaks in the deconvoluted spectrum, mAb-A is primarily G0F/G0F and G0F/G1F at 77.2% and 18.3%, respectively. The remaining glycoforms account for less than 5% each: 2.5% G2F, 1.7% G0, 0.2% G0F(-GlcNAc), and 0.1% partially aglyco mAb. Results from conventional glycan cleavage and derivatization analysis support the identification of the intact glycoforms. However, as seen in Table S2, there are low abundance glycans (less than 0.15% of total population) detected through the cleaved glycan analysis that are not identified in the deconvoluted mass spectrum. These species differ in mass from one of the identified glycoforms by less than 50 Da and are spectrally obscured by the more abundant species. For instance, Man 5 differs in mass by 23 Da from G0F(-GlcNAc) and G1F(-GlcNAc) differs from G0F by 36 Da. At such low abundances these species will not be resolved in the mass domain without a mass spectrometer with higher resolving power. Although some minor glycoforms are not resolved in the mass domain, this method is able to detect aglyco isoforms of the mAb, which is information that is not generated through cleaved glycan analysis. Additionally, this glycoform information can be generated in minutes with minimal sample preparation as no enzymatic digestion and labeling is required.

Analysis of mAb-Ac Variants. mAb-Ac was created by collaborators at Pfizer using previously described conjugation chemistry that attaches the drug compound to the sidechain of lysine residues in mAb-A.[40] The drug conjugated to the antibody is primarily neutral, and therefore the main shifts in the pI of the intact ADC are associated with the loss of available ε-amino groups in the lysine residues that are conjugated. As such, this reaction would decrease the mobility as the DAR increases. Additionally, it is reasonable to expect each mAb-Ac conjugate species to maintain the initial charge variant and glycoform profile of the starting molecule, mAb-A (Figure. 2a). Intact charge variant analysis of mAb-Ac is provided in Figure 3 along with the identified glycoforms from the deconvoluted mass spectrum of the most abundant charge variant. Five DAR species are detected and labeled with the mass obtained from deconvoluting the mass spectrum generated from each band. The minor basic variants associated with each are the previously identified pyroglutamic acid variants found in mAb-A. Although the signal intensity for DAR 4 is low, a peak is present in the extracted ion electropherogram for that species (Figure S1).

The deconvoluted mass spectra from each of the separated DAR species and the mass shift between each species is provided in Figure 4. The average mass shift due to an increase in DAR is 3145 Da, which agrees very well with the known mass of the drug load. Migration times and mobilities for the mAb-Ac DAR species can be found in Table S3. Although the addition of a drug load should only decrease the net charge on the mAb by 1 unit, a more substantial shift in

mobility of $0.1x10^{-4}$ cm^2/Vs is observed than previously calculated for modifications causing a similar change in net charge.[28] This is most likely due to the size of the drug load. At 3145 Da, this mass accounts for approximately 2% of the total mAb mass per drug load. This is a much larger mass shift compared to those associated with C-terminal lysine truncations or pyroglutamic acid formation. It can be surmised that the presence of a drug load(s) on the mAb structure affects the hydrodynamic radius of the molecule in solution, which in turn affects the mobility of the mAb.

The mass of DAR 0 in Figure 3 is similar to the mass calculated for mAb-A (Figure. 2a) but is not identical and the migration times vary slightly. To determine whether these minor variations are caused by additional modification to the mAb-A structure during the conjugation reaction or simply the result of experimental variability, 5 µg of mAb-A was spiked into the mAb-Ac sample. Multiple bands would be expected in the region of DAR 0 if this species differed from mAb-A. However, as seen in Figure 5, DAR 0 and its associated variants increased in intensity after mAb-A was spiked into the sample. Additionally, there are no partially resolved variants appearing as shoulders in the area of DAR 0 or protein envelopes present in the mass spectrum that were not there previously. Thus, DAR 0 in mAb-Ac can be confirmed to be residual mAb-A in the sample.

Drug Load Distribution. To establish that the dynamic range of the mass spectrometer was sufficient to calculate DAR distribution, a range of mAb-Ac concentrations were analyzed using the microfluidic CE-MS method. The areas for each DAR species were calculated using MassLynx software and plotted against the sample concentration (Figure. S2). The MS response was found to be linear for all DAR species at less than 1.5 mg/mL mAb-Ac. Representative calculations for determining DAR distribution are provided in the Supporting Information. The relative area percent (corrected for injection bias) was calculated for each DAR species in the separation and is provided in Table 2. The average DAR was found to be 1.7. An infusion of mAb-Ac performed by opening the microchip gate valve as mentioned above and the relative area percent of the DAR species is provided in Table 2. The results of the infusion also yielded an average DAR of 1.7. Both the CE-MS and infusion values are in relative agreement with conventional analytical methods that measure the DAR of ADCs. Table 2 also lists the distribution of DAR species calculated from imaging CE (iCE) data collected by collaborators at Pfizer where an average DAR value of 1.8 was obtained.

Table 2: Area percent of DAR species generated via microfluidic CE-MS, infusion-MS, and iCE.

Species	CE-MS Area %	Infusion Area %	iCE Area %
DAR-0	7.2%	8.6%	5.8%
DAR-1	30.2%	33.2%	29.1%
DAR-2	46.4%	39.0%	44.8%
DAR-3	14.0%	16.5%	16.7%
DAR-4	2.3%	2.7%	3.6%

While the drug load distribution generated using the CE-MS and infusion methods is similar, more information is generated about the charge heterogeneity of the mAb-Ac population through the intact charge variant analysis. Figure 6 compares the raw mass spectra for the DAR 2 variants in the infusion data and the separation in Figure 3. The mass difference of 18 Da associated with the pyroglutamic acid variants was not resolved in the mass domain during the mAb-Ac infusion experiment. As indicated in Figure 6b, there is a slight mass shift discernable between the spectra for the 2 load variant with and without pyroglutamic acid, but this shift only manifests as spectral broadening in the infusion spectrum. When deconvoluted, the mass obtained from the infusion data is a function of the mass of both pyroglutamic acid variants.

ADC Conformational Isomers. It is evident from the data provided that at least four sites on the intact mAb-A structure readily undergo conjugation during the reaction Although IgG type antibodies consist of two heavy chains and two light chains, the overall molecule is not conformationally symmetric[7] and the occurrence of a drug load at the same residue but on different chains may have different structural effects that could affect the mobility. Thus, there are positional isomers determined by the location and identity of the conjugation site accessed, which could perturb the mAb structure enough to affect the mobility on the basis of conformation. Potential evidence for this is present as reproducible shoulder features on DAR species 1 and 2 in the electropherogram for mAb-Ac. These features are marked with asterisks in Figure 3. The mass spectra are homogenous throughout the width of both bands indicating that the partially resolved shoulder species do not differ in mass. If the resolution of the CE separation were increased it is possible that these isomers could be separated and used to further assess the conjugation reaction based on drug load location in addition to DAR.

CONCLUSIONS

In this work we have demonstrated the use of microfluidic CE-ESI with online MS analysis for the characterization of intact antibody drug conjugates. This analysis method appears to be a simple, generic strategy for characterizing the charge heterogeneity of mAbs and ADCs with direct MS analysis. Intact charge variant analysis of the base mAb revealed the presence of pyroglutamic acid and decarboxylated variants along with various glycoforms of antibody. These variants were confirmed by both mass shifts and changes in the mobility of the species. Post conjugation, these variants were present in the resulting mAb-Ac sample in addition to DAR variants. The average DAR and DAR distribution for mAb-Ac was assessed based on the resulting electropherogram. Five separate mAb-Ac species with different DARs were detected from the separation and mass spectral data with an average mass shift of 3145 Da. It was determined that a maximum of 4 drug loads were present on the mAb with an average DAR of 1.7. While the addition of a drug load should theoretically only reduce the mAb net charge by 1 unit, a relatively large decrease in mobility was seen due to conjugation. This is most likely

attributable to changes in the hydrodynamic radius of the molecule induced by the size of the drug load. It was postulated that partial separation of conformational isomers was seen due to the band widths of DAR species 1-3 and reproducible shoulder features in the electropherogram. The mobility differences between such conformational isomers would be less than those caused by charge differences and more difficult to resolve in the CE domain. Altering the background electrolyte or increasing the operating voltage could potentially increase the separation resolution and confirm or refute the presence of structural isomers. Additional experiments are being done to explore this possibility.

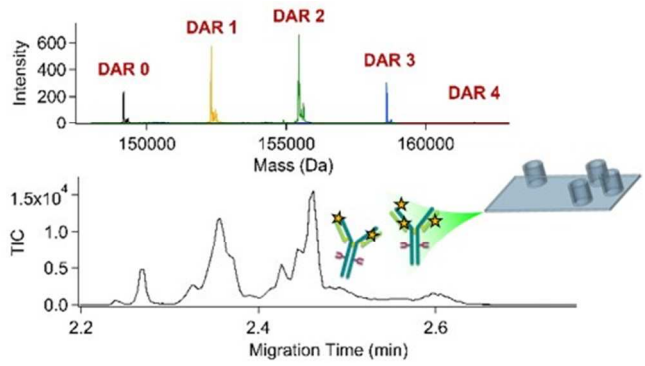
The properties of the ADC drug load and the type of conjugation chemistry used can significantly affect the charge heterogeneity of the ADC species. For instance, a cationic drug load would negate the decrease in net charge associated with lysine conjugation and separation of DAR species would be dependent on conformational changes. For smaller drug loads this could make separation of the DAR species quite challenging. Currently, experiments are being performed to assess the utility of this method for analyzing ADCs with smaller molecule drug loads and different conjugation chemistry, such as cysteine linked ADCs.

Acknowledgments

We would like to thank the National Institutes of Health (Grant 5R01GM066018-11) and the University of North Carolina at Chapel Hill Center for Biomedical Microdevices for funding of this project.

Supporting Information Available: Additional information about the migration time reproducibility, glycan identification, cleaved glycan analysis, and DAR calculation is provided. This material is available free of charge via the Internet at http://pubs.acs.org.

For TOC only



REFERENCES

(1) Wakankar, A.; Chen, Y.; Gokarn, Y.; Jacobson, F. S. *MAbs* **2011**, *3* (2), 161–172.

(2) Alley, S. C.; Anderson, K. E. *Curr. Opin. Chem. Biol.* **2013**, *17* (3), 406–411.

(3) Teicher, B. a.; Chari, R. V. J. *Clin. Cancer Res.* **2011**, *17* (20), 6389–6397.

(4) Le, L. N.; Moore, J. M. R.; Ouyang, J.; Chen, X.; Nguyen, M. D. H.; Galush, W. J. *Anal. Chem.* **2012**, *84* (17), 7479–7486.

(5) Ducry, L. *Antibody-Drug Conjugates*; Springer: New York, NY, 2013.

(6) Flygare, J. A.; Pillow, T. H.; Aristoff, P. *Chem. Biol. Drug Des.* **2013**, *81* (1), 113–121.

(7) Liu, H.; Gaza-bulseco, G.; Faldu, D.; Chumsae, C.; Sun, J. *J. Pharm. Sci.* **2008**, *97*, 2426–2447.

(8) Macht, M. *TrAC Trends Anal. Chem.* **2013**, *48*, 62–71.

(9) Zhang, H.; Cui, W.; Gross, M. L. *FEBS Lett.* **2014**, *588* (2), 308–317.

(10) Zhang, Z.; Pan, H.; Chen, X. *Mass Spectrom. Rev.* **2009**, *28*, 147–176.

(11) Khawli, L. A.; Goswami, S.; Hutchinson, R.; Kwong, Z. W.; Yang, J.; Wang, X.; Yao, Z.; Sreedhara, A.; Cano, T.; Tesar, D. B.; Nijem, I.; Allison, D. E.; Wong, P. Y.; Kao, Y.-H.; Quan, C.; Joshi, A.; Harris, R. J.; Motchnik, P. *MAbs* **2010**, *2* (6), 613–624.

(12) Strop, P.; Delaria, K.; Foletti, D.; Witt, J. M.; Hasa-Moreno, A.; Poulsen, K.; Casas, M. G.; Dorywalska, M.; Farias, S.; Pios, A.; Lui, V.; Dushin, R.; Zhou, D.; Navaratnam, T.; Tran, T.-T.; Sutton, J.; Lindquist, K. C.; Han, B.; Liu, S.-H.; Shelton, D. L.; Pons, J.; Rajpal, A. *Nat. Biotechnol.* **2015**, *33* (7), 694–696.

(13) Lyon, R. P.; Bovee, T. D.; Doronina, S. O.; Burke, P. J.; Hunter, J. H.; Neff-LaFord, H. D.; Jonas, M.; Anderson, M. E.; Setter, J. R.; Senter, P. D. *Nat. Biotechnol.* **2015**, *33* (7), 733–735.

(14) Fekete, S.; Beck, A.; Veuthey, J.-L.; Guillarme, D. *J. Pharm. Biomed. Anal.* **2015**, 1–13.

(15) Harrington, S.; Varro, R.; Li, T. *J. Chromatogr.* **1991**, *559*, 385–390.

(16) Krull, I. S.; Liu, X.; Dai, J.; Gendreau, C.; Li, G. *J. Pharm. Biomed. Anal.* **1997**, *16* (3), 377–393.

(17) Xu, K.; Liu, L.; Saad, O. M.; Baudys, J.; Williams, L.; Leipold, D.; Shen, B.; Raab, H.; Junutula, J. R.; Kim, A.; Kaur, S. *Anal. Biochem.* **2011**, *412* (1), 56–66.

(18) Michels, D. a.; Salas-Solano, O.; Felten, C. *Bioprocess Int.* **2011**, *9* (10), 48–54.

(19) Chen, X.; Nguyen, M.; Jacobson, F.; Ouyang, J. *MAbs* **2009**, *1* (6), 563–571.

(20) Birdsall, R. E.; Shion, H.; Kotch, F. W.; Xu, A.; Porter, T. J.; Chen, W. *MAbs* **2015**, *0862* (December), 1–9.

(21) Hamblett, K. J.; Senter, P. D.; Chace, D. F.; Sun, M. M. C.; Lenox, J.; Cerveny, C. G.; Kissler, K. M.; Bernhardt, S. X.; Kopcha, A. K.; Zabinski, R. F.; Meyer, D. L.; Francisco, J. a. *Clin. Cancer Res.* **2004**, *10* (425), 7063–7070.

(22) Roman, G. T.; Shion, H.; Murphy, J. P.; Chen, W. *Waters Corp. Appl. Note* **2015**, No. 720005378EN.

(23) Alvarez, M.; Tremintin, G.; Wang, J.; Eng, M.; Kao, Y.-H.; Jeong, J.; Ling, V. T.;

Borisov, O. V. *Anal. Biochem.* **2011**, *419*, 17–25.

(24) Bondarenko, P. V; Second, T. P.; Zabrouskov, V.; Makarov, A. a; Zhang, Z. *J. Am. Soc. Mass Spectrom.* **2009**, *20* (8), 1415–1424.

(25) Marcoux, J.; Champion, T.; Colas, O.; Wagner-Rousset, E.; Corvaïa, N.; Van Dorsselaer, A.; Beck, A.; Cianférani, S. *Protein Sci.* **2015**.

(26) Debaene, F.; Wagner-rousset, E.; Colas, O.; Ayoub, D.; Corva, N.; Dorsselaer, A. Van; Beck, A.; Cianferani, S. *Anal. Chem.* **2013**, *85*, 9785–9792.

(27) Debaene, F.; Amandine, B.; Wagner-rousset, E.; Colas, O.; Ayoub, D.; Corva, N.; Dorsselaer, A. Van; Beck, A.; Cianfe, S. *Anal. Chem.* **2014**, *86*, 10674–10683.

(28) Redman, E. A.; Batz, N. G.; Mellors, J. S.; Ramsey, J. M. *Anal. Chem.* **2015**, *87* (4), 2264–2272.

(29) Batz, N. G.; Mellors, J. S.; Alarie, J. P.; Ramsey, J. M. *Anal. Chem.* **2014**, *86*, 3493–3500.

(30) Culbertson, C. T.; Jacobson, S. C.; Ramsey, J. M. *Anal. Chem.* **2000**, *72* (23), 5814–5819.

(31) Culbertson, C. T.; Jacobson, S. C.; Ramsey, J. M. *Anal. Chem.* **1998**, *70*, 3781–3789.

(32) Jacobson, S. C.; Hergenroder, R.; Koutny, L. B.; Ramsey, J. M. *Anal. Chem.* **1994**, *66*, 1114–1118.

(33) Jacobson, S. C.; Mcknight, T. E.; Ramsey, J. M. *Anal. Chem.* **1999**, *71* (20), 5172–5176.

(34) Jacobson, S. C.; Hergenroder, R.; Koutny, L. B.; Warmack, R. J.; Ramsey, J. M. *Anal. Chem.* **1994**, *66*, 1107–1113.

(35) Mellors, J. S.; Gorbounov, V.; Ramsey, R. S.; Ramsey, J. M. *Anal. Chem.* **2008**, *80* (18), 6881–6887.

(36) Mellors, J. S.; Jorabchi, K.; Smith, L. M.; Ramsey, J. M. *Anal. Chem.* **2010**, *82* (3), 967–973.

(37) Jacobson, S. C.; Koutny, L. B.; Hergenroder, R.; Moore, A. W.; Ramsey, J. M. *Anal. Chem.* **1994**, *66* (20), 3472–3476.

(38) Berger, S. J.; Chen, W. *Waters Corporation Application Note*. 2008, p Number APNT10094155.

(39) Ferrige, A. G.; Seddon, M. J.; Green, B. N.; Jarvix, S. A.; Skilling, J. *Rapid Commun. Mass Spectrom.* **1992**, *6*, 707–711.

(40) Doppalapudi, V. R.; Huang, J.; Liu, D.; Jin, P.; Liu, B.; Li, L.; Desharnais, J.; Hagen, C.; Levin, N. J.; Shields, M. J.; Parish, M.; Murphy, R. E.; Del Rosario, J.; Oates, B. D.; Lai, J.-Y.; Matin, M. J.; Ainekulu, Z.; Bhat, A.; Bradshaw, C. W.; Woodnutt, G.; Lerner, R. a; Lappe, R. W. *Proc. Natl. Acad. Sci. U. S. A.* **2010**, *107* (52), 22611–22616.

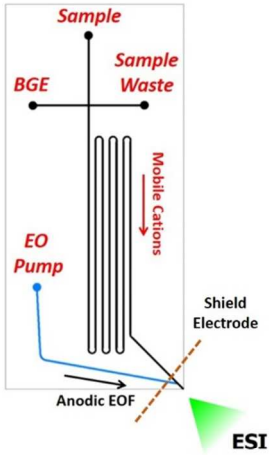


Figure 1: Schematic of microfluidic CE-ESI device used for this work. Black channels indicate an APS-PEG coating and blue channels indicate an APS coating.

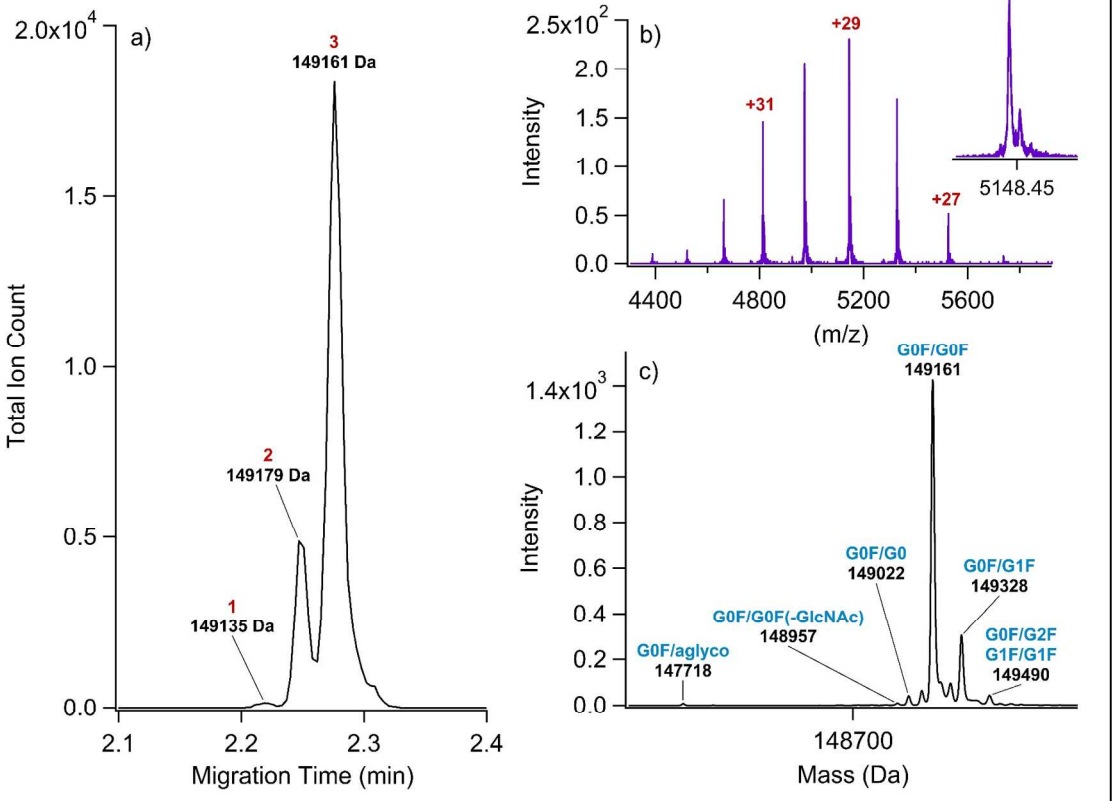


Figure 2: Characterization of mAb-A: a) Electropherogram of intact charge variants generated via microfluidic CE-ESI-MS. Peaks are labeled with the mass obtained through deconvolution of that variants' mass spectra. b) Raw mass spectrum corresponding to the most abundant charge variant, c) Deconvolution of the mass spectrum in b with identifiable glycoforms labeled.

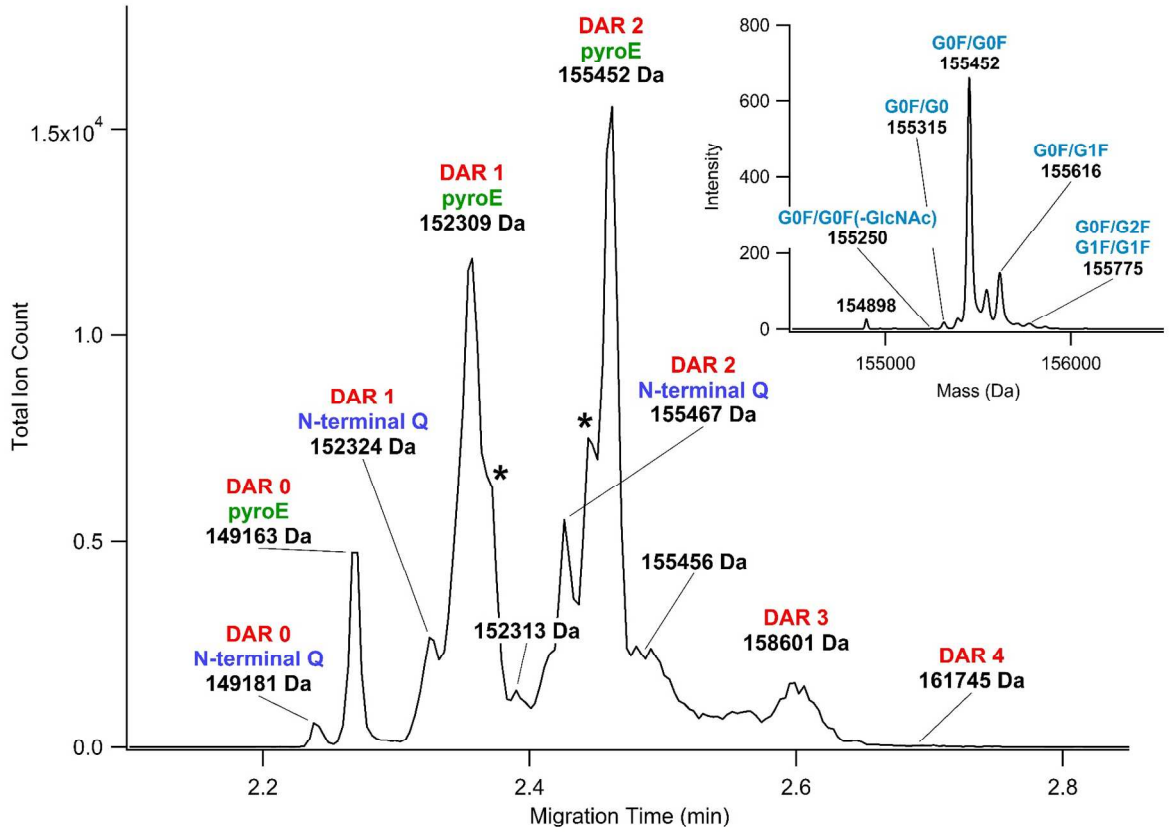


Figure 3: Intact charge variant separation of mAb-Ac. Peaks are labeled with masses obtained by deconvolution of the mass spectrum associated with that peak. Pyroglutamic acid variants of each DAR species are labeled as having either an N-terminal Q or pyroE. (*) indicate reproducible shoulder features on the main peaks. The inset shows the deconvoluted mass spectrum for DAR 2 with identified glycoforms labeled.

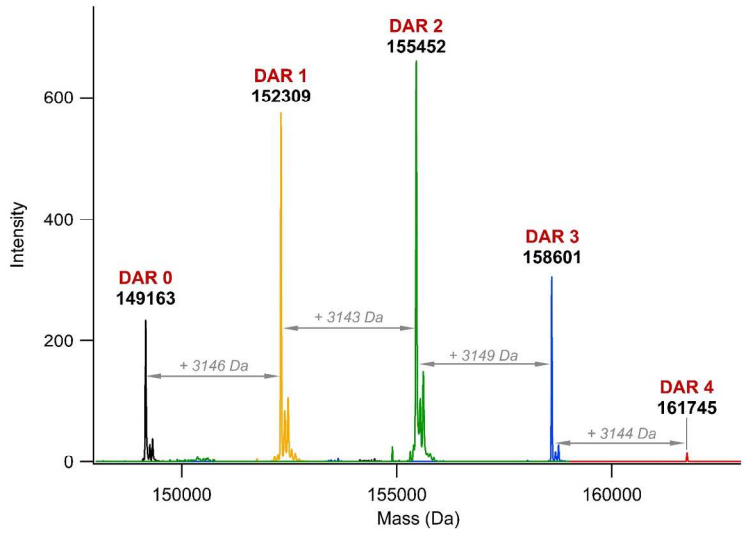


Figure 4: Overlaid deconvoluted mass spectra for DAR species 0-4 generated from the electropherogram shown in Figure 3. The mass shift between neighboring DAR species is shown with an average mass shift calculated at 3145 Da.

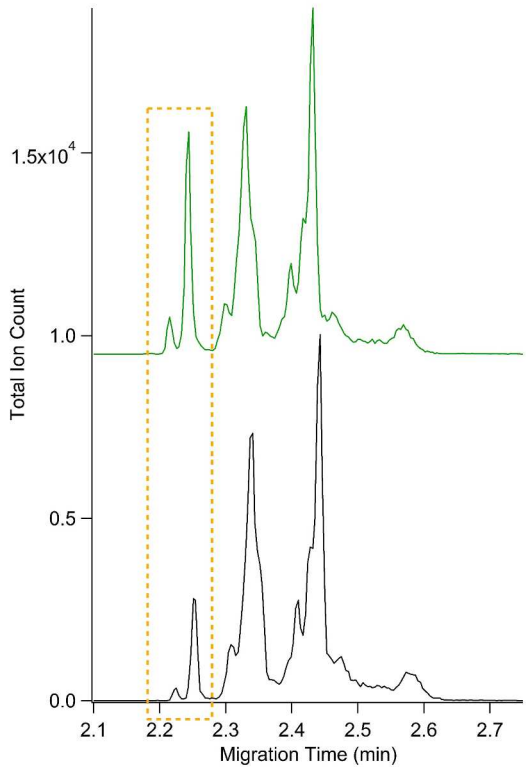


Figure 5: Intact charge variant analysis of mAb-Ac (bottom) and mAb-Ac spiked with mAb-A (top). The intensity of the peaks highlighted in the box increases after the sample is spiked with mAb-A.

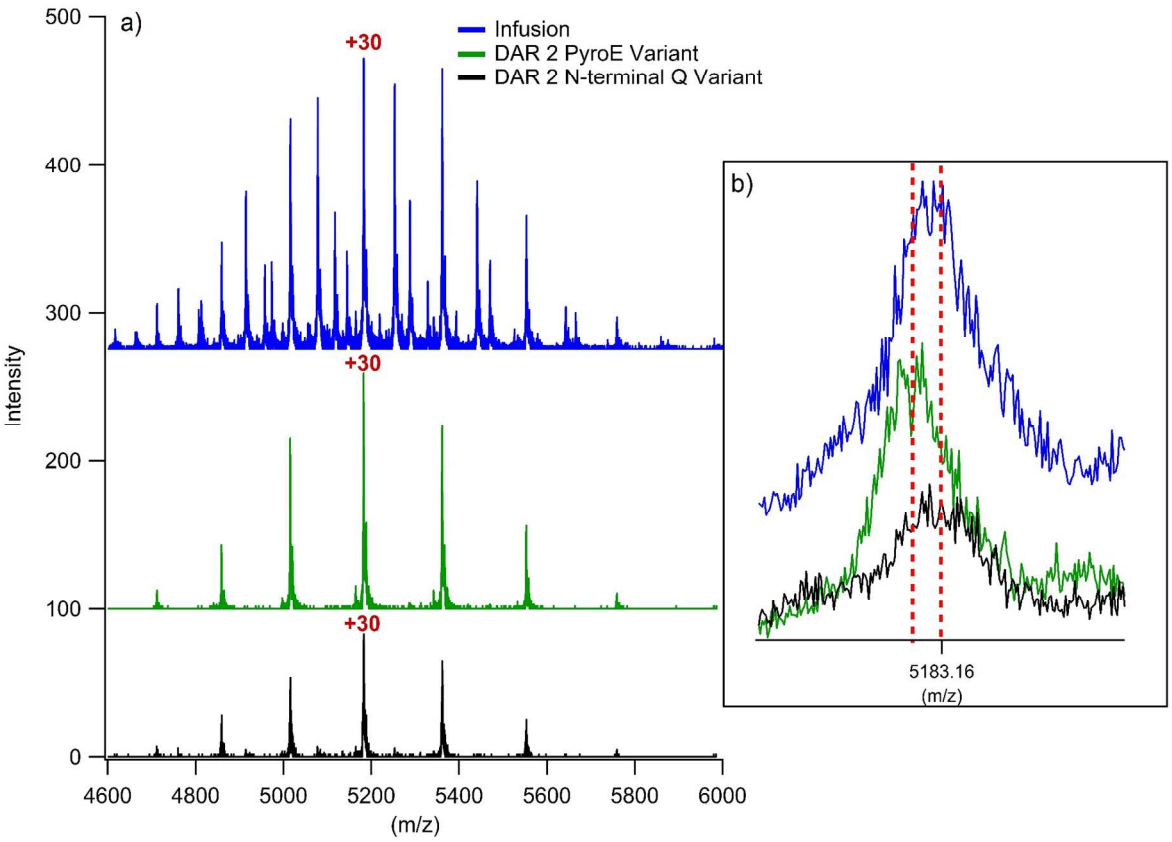


Figure 6: Comparison of infusion-MS and intact CE-ESI-MS analysis: a) mass spectrum of the pyroglutamic acid and N-terminal Q variants of the DAR 2 species (green, black) compared to an infusion of mAb-Ac containing all DAR species (blue). b) comparison of the +30 charge states of the DAR 2 species in the infusion spectrum and separation spectra. The 18 Da mass shift due to the cyclization of glutamine is not resolved in the infusion spectrum.